

## Research Article

# High-Performance Biocomposite Polyvinyl Alcohol (PVA) Films Modified with Cellulose Nanocrystals (CNCs), Tannic Acid (TA), and Chitosan (CS) for Food Packaging

Ruowen Tan,<sup>1</sup> Feng Li,<sup>2</sup> You Zhang,<sup>1</sup> Zihui Yuan,<sup>1</sup> Xuefei Feng,<sup>3</sup> Wansong Zhang,<sup>1</sup> Ting Liang,<sup>1</sup> Jiwen Cao,<sup>1</sup> Cornelis F. De Hoop,<sup>4</sup> Xiaopeng Peng ,<sup>5</sup> and Xingyan Huang <sup>1</sup>

<sup>1</sup>College of Forestry, Sichuan Agricultural University, Chengdu, Sichuan 611130, China

<sup>2</sup>Landscape Architecture School, Chengdu Agricultural College, Chengdu, Sichuan 611130, China

<sup>3</sup>Department of Stomatology, North Sichuan Medical University, Nanchong 637007, China

<sup>4</sup>School of Renewable Natural Resources, Louisiana State University Agricultural Center, Baton Rouge, LA 70803, USA

<sup>5</sup>State Key Laboratory of Tree Genetics and Breeding, Key Laboratory of Tree Breeding and Cultivation of the National Forestry and Grassland Administration, Research Institute of Forestry, Chinese Academy of Forestry, Beijing 100091, China

Correspondence should be addressed to Xiaopeng Peng; xp@caf.ac.cn and Xingyan Huang; hxy@sicau.edu.cn

Received 27 July 2021; Revised 28 September 2021; Accepted 2 November 2021; Published 17 December 2021

Academic Editor: Leander Tapfer

Copyright © 2021 Ruowen Tan et al. This is an open access article distributed under the Creative Commons Attribution License, which permits unrestricted use, distribution, and reproduction in any medium, provided the original work is properly cited.

Polyvinyl alcohol (PVA) has been widely applied in industries for its low cost, nontoxicity, biodegradability, and renewable advantages. However, its unstable structure may not meet some strong physical and mechanical needs. In order to enhance the performances of the PVA film, cellulose nanocrystals (CNCs), tannic acid (TA), and chitosan (CS), working as a reinforcer, a crosslinker, and an antimicrobial agent, respectively, were introduced into the PVA matrix. The results indicated that CNCs, TA, and CS were evenly distributed and cohesively incorporated within the PVA matrix, which contributed to the good mechanical properties and thermal stabilities of biocomposite PVA films. Besides, the addition of TA remarkably improved the antiultraviolet and antioxidant capabilities of PVA films, although the light transmittance declined slightly. It was also observed that the pure PVA film and PVA reinforced with CNCs were incapable of protecting against bacteria, while the ones with CS had prominent antibacterial properties to *Escherichia coli* and *Staphylococcus aureus*. Overall, the resulting film presented a high potential utilization as a food packaging material for its outstanding physical and mechanical performances.

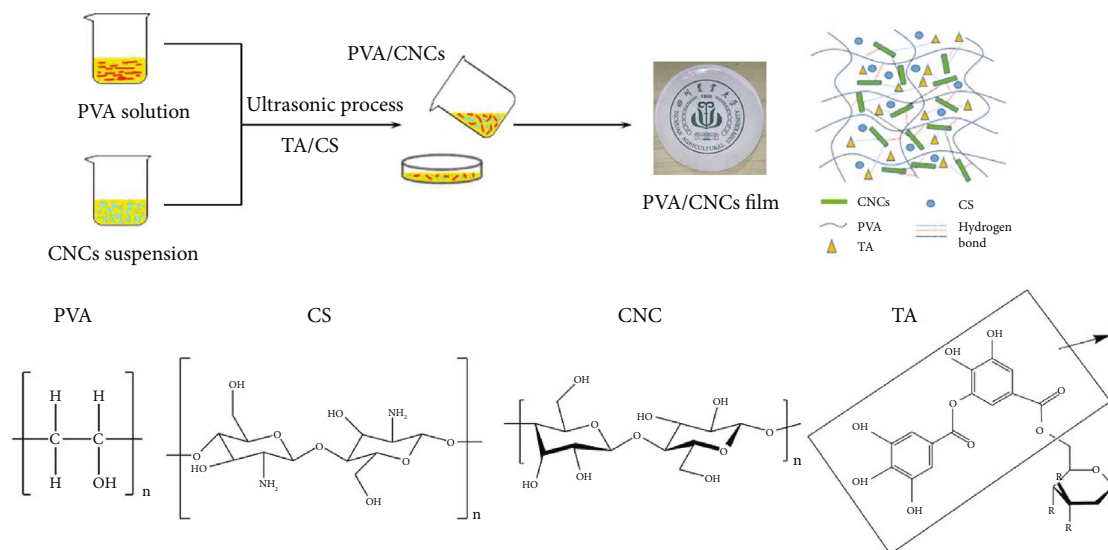
## 1. Introduction

The traditional fossil fuel-based synthetics had caused serious problems to environment for their nondegradability and the waste accumulation in nature [1]. In order to mitigate these environmental problems, adopting renewable biomaterials in food packaging was regarded as an effective protection technique due to their virtues in the biodegradability, antibacterial ability, nontoxicity, and low cost [2].

Polyvinyl alcohol (PVA) is a synthetic polymer with a broad application in industrial areas, such as drug delivery, recycling polymers, film formation, and food packaging [3–7]. Due to the large amount of hydroxyl groups on the PVA carbon chain, the formation of the polymer complex

could be enhanced through hydrogen bonding [8]. It also has a high water vapor permeability because of its extreme hydrophilicity [9]. However, the thin PVA film has poor mechanical properties and antibacterial abilities. The excellent mechanical, antibacterial, and antiultraviolet properties are crucial to food packaging material. Therefore, it is essential to boost the physical and mechanical performances of PVA. In this work, therefore, a reinforcer, a crosslinker, and an antibacterial agent were introduced to build a PVA-based complex.

Cellulose nanocrystals (CNCs) are an ideal reinforcer in biopolymer industries [4, 10]. The main advantages of CNCs include low density, positive ecological effect, and easy recycling and processing ability [11]. It is easy to adjust



SCHEME 1: The preparation process of biocomposite PVA films with CNCs, TA, and CS.

properties and broaden applications of CNCs by modifying its surface hydroxyl groups [12]. With the functionalization of covalent and noncovalent frameworks, the modified CNCs are beneficial to dispersion for improving the compatibility with the polymer matrix [13, 14]. There has been a growing interest in researches about PVA films reinforced by CNCs in the last few years, such as CNC-modified biodegradable packaging materials [15, 16].

Tannic acid (TA) is a gallic ester of D-glucose with low cost, biodegradability, and nontoxicity [17, 18]. TA was found to be very useful as a surface coating material to form TA polymeric layers on various substrates in polymerization [19]. Due to its multiple phenolic groups that can interact with biological macromolecules, it has excellent antioxidant properties. As a crosslinker, it has a tendency to form more stable structure owing to the reorganization toward an anhydrous conformation [20]. Besides, it has been used as a crosslinker in gelatin films, enhancing the conjunction of the hydrogen bonding between gelatin and TA molecules [21]. In a word, TA is a good choice to produce a biocomposite for its natural product extracted from plants in a low cost [22].

Chitosan (CS) is nontoxic and renewable. Thus, it has various applications, such as pharmaceutical, medical, and food fields [23]. It is composed of linear polysaccharide in its molecular chain [24]. Its antibacterial activity was mainly influenced by the number of  $\text{NH}_2$  groups [25]. The antimicrobial chitosan is a prominent agent on the basis of the functional group conjugated to the polymer backbone [26].

In order to enhance the physical and mechanical properties of PVA, i.e., antiultraviolet capability, antioxidant property, thermal stability, tensile strength, and antibacterial ability, CNCs, TA, and CS were used as a reinforcer, a crosslinker, and an antibacterial agent in the present work. The preparation process of resulting biocomposite PVA films modified by CNCs, TA, and CS is illustrated in Scheme 1.

## 2. Materials and Methods

**2.1. Materials.** Polyvinyl alcohol (PVA) was purchased from Guangdong Fine Chemical Engineering Technology Research and Development Center (Shantou City, China). Cellulose nanocrystals (CNCs) were supplied as 8.0% *w/w* aqueous suspension, from BGB Ultra, Canada. Tannic acid (TA) was purchased from Tianjin Chemical Reagents Ltd. (Tianjin City, China). Chitosan (CS) was obtained from Sinopharm Chemical Reagent Co., Ltd. DPPH was provided by Shanghai Yuanye Bio-Technology Co., Ltd. All chemicals were used without further purification.

**2.2. Preparation of Resulting Biocomposite PVA Films.** As shown in Scheme 1, PVA was dissolved in hot distilled water (85°C) to make the 5%wt PVA solution. Then, CNCs (1%wt, 3%wt, 5%wt, 7%wt, and 9%wt) were dispersed to reinforce the PVA matrix. TA (2%wt, 4%wt, 6%wt, 8%wt, and 10%wt), as a crosslinker, was added into the solution with a constant stirring and heating. Thereafter, CS (5%wt, 10%wt, and 20%wt, dissolved in 1% acetic acid) was applied to increase the antibacterial ability of PVA films. The proportions of CNCs, TA, and CS were calculated referring to the initial PVA weight. It was notable that the whole preparation process was required to guarantee no water loss or evaporation. After completing the synthesis procedure, the resulting solution finally was poured into plates to evaporate redundant water at room temperature. The labels of resulting biocomposite films with different amounts of components were marked by PVA/%CNCs/%TA/%CS.

### 2.3. Characterizations

**2.3.1. Mechanical Properties.** Tensile strength and elongation at break of PVA films were performed to evaluate their mechanical properties, using an Instron (electronic universal tensile testing machine, FBS-1000N). Tensile strength was defined as the maximum strength of breaking out, while elongation at break was calculated by dividing the extension

TABLE 1: The effect of different ratios (PVA/CNCs/TA/CS) on the tensile strength and elongation at break of PVA films.

Films	Tensile strength (MPa)	Elongation at break (%)
PVA	34.6 ± 1.4 <sup>a</sup>	37.6 ± 5.8 <sup>a</sup>
PVA/1%CNC	47.3 ± 2.1 <sup>ab</sup>	63.0 ± 8.3 <sup>b</sup>
PVA/3%CNC	58.9 ± 2.3 <sup>b</sup>	73.8 ± 10.5 <sup>c</sup>
PVA/5%CNC	63.6 ± 5.7 <sup>b</sup>	113.5 ± 10.2 <sup>d</sup>
PVA/7%CNC	62.7 ± 7.4 <sup>b</sup>	101.4 ± 13.6 <sup>d</sup>
PVA/9%CNC	47.3 ± 3.5 <sup>ab</sup>	71.0 ± 7.1 <sup>c</sup>
PVA/5%CNC/2%TA	66.1 ± 5.8 <sup>b</sup>	14.3 ± 3.2 <sup>e</sup>
PVA/5%CNC/4%TA	68.3 ± 4.7 <sup>bc</sup>	29.8 ± 3.8 <sup>f</sup>
PVA/5%CNC/6%TA	70.6 ± 4.1 <sup>c</sup>	26.4 ± 4.9 <sup>f</sup>
PVA/5%CNC/8%TA	71.8 ± 5.2 <sup>c</sup>	54.8 ± 9.6 <sup>b</sup>
PVA/5%CNC/10%TA	75.5 ± 3.7 <sup>c</sup>	5.4 ± 1.7 <sup>g</sup>
PVA/5%CNC/8%TA/5%CS	55.9 ± 3.9 <sup>b</sup>	33.9 ± 6.0 <sup>a</sup>
PVA/5%CNC/8%TA/10%CS	58.5 ± 5.2 <sup>b</sup>	28.8 ± 3.2 <sup>f</sup>
PVA/5%CNC/8%TA/20%CS	63.0 ± 6.4 <sup>b</sup>	2.0 ± 0.7 <sup>g</sup>

Note: means with the same letter in the same column are not significantly different at the 0.05 probability level.

length at fracture by the initial length of the films and expressed as a percentage result. The samples were made into strips, 10 × 50 mm with thickness of 0.3 ± 0.1 mm. The initially separated distance and speed were set as 30 mm and 2 mm/min, respectively. The results of tensile strength and elongation at break were the averages of 6 tests.

**2.3.2. Scanning Electron Microscope (SEM).** The surface morphologies of prepared samples were examined *via* SEM (TESCAN MIRA4).

**2.3.3. Fourier Transform Infrared Spectroscopy (FTIR).** The chemical structures of PVA films were investigated by FTIR on a Nicolet IS 10 spectrometer (Thermo Fisher Scientific, MA, USA). A small quantity of samples was covered flatwise on the detection window. The measurement was achieved from 400 cm<sup>-1</sup> to 4000 cm<sup>-1</sup> with a spectral resolution of 4 cm<sup>-1</sup>, and a total of 32 scans were collected.

**2.3.4. X-Ray Diffraction (XRD).** The degree of crystallinity is very important, for it defines the physical and mechanical properties of the composite system [27]. An X-ray diffraction pattern was tested using a Bruker Siemens D5000 X-ray automated powder X-ray diffractometer (Siemens Co., Wittelsbacherplatz, Munich, Germany) at ambient temperature. The detection was performed at a scan speed of 2°/min over the 2θ from 3 to 50° with Cu-Kα radiation (λ = 1.5406 Å) at 45 kV and 40 mA.

**2.3.5. Thermal Activities.** The thermogravimetric/differential thermogravimetric (TG/DTG) analysis and differential scanning calorimetry (DSC) were carried out by using a simultaneous thermal analysis TG-DSC (TA Instruments, New Castle, DE). Approximately 3 mg sample was heated from 25 to 800°C at the heating rate of 10°C/min. The measurements were processed under a nitrogen atmosphere with

gas flow of 50 mL/min. The differential scanning temperature was from 50 to 250°C with a heating rate of 10°C/min under a nitrogen atmosphere.

**2.3.6. UV-vis Spectroscopy.** The antiultraviolet abilities of PVA films were evaluated by using a HP UV-vis spectrophotometer (UNICO UV-4802H), working in the wavelength between 190 and 800 nm.

**2.3.7. Antioxidant Properties.** The antioxidant activity of PVA films was evaluated by the modified methods according to Liu et al. [28]. Approximately 100 mg of film pieces was mixed with 95% ethanol. The films were added into the DPPH (0.1 mM DPPH radical in an aliquot of the 95% ethanolic solution), which also was set as the initial control at wavelength 515 nm performed on a HP UV-vis spectrophotometer (UNICO UV-4802H). Samples should be retained in the dark at room temperature for 30 minutes. The tests were in triplicate, and the antioxidant property of PVA biocomposite films was expressed as percent inhibition of the DPPH radical (DPPH inhibition %), calculated according to.

$$\text{DPPH inhibition(\%)} = \left( \frac{A_0 - A_1}{A_0} \right) \times 100, \quad (1)$$

where  $A_0$  is the absorbance of the DPPH radical and  $A_1$  is the absorbance of the sample.

**2.3.8. Antibacterial Properties.** The antibacterial properties of PVA films were evaluated by the agar diffusion method against Gram-negative *Escherichia coli* and *Staphylococcus aureus*. Film samples were prepared as 15 mm in diameter. The *Escherichia coli* and *Staphylococcus aureus* were inoculated into the Lysogeny broth and cultivated at 37°C for 24 h. Then, the bacteria were diluted with sterile water into 10<sup>8</sup> CFU/mL, before placing them into a nutrient agar plate. The incubation should be continued at 37°C for 24-48 h. Finally, the discs of inhibitory districts surrounding films were tested as indications of antibacterial activities against *Escherichia coli* and *Staphylococcus aureus*.

### 3. Results and Discussion

**3.1. Mechanical Properties.** The mechanical properties of biocomposite PVA films are shown in Table 1. It was worth noting that all biocomposite PVA films had higher tensile strengths than the pure one. The tensile strength and elongation at break of PVA were reinforced by CNCs, which were partially ascribed to the high crystallinity of CNCs with the enhancement of inherent chain stiffness and rigidity [29]. Furthermore, the hydrophilicity (functioning as a carrier of water) of CNCs could slightly plasticize the PVA matrix, resulting in a better ductility and elongation at break [30]. However, as the CNC dosage was over 5%, the tensile strength and elongation at break decreased. It was mainly due to the agglomeration of CNCs, which could reduce the valid reinforcement [31]. Therefore, 5% CNCs were optimized to reinforce the PVA matrix, where the maximum tensile strength and elongation at break of the PVA film reinforced by CNCs were 63.6 MPa and 113.5%, respectively.

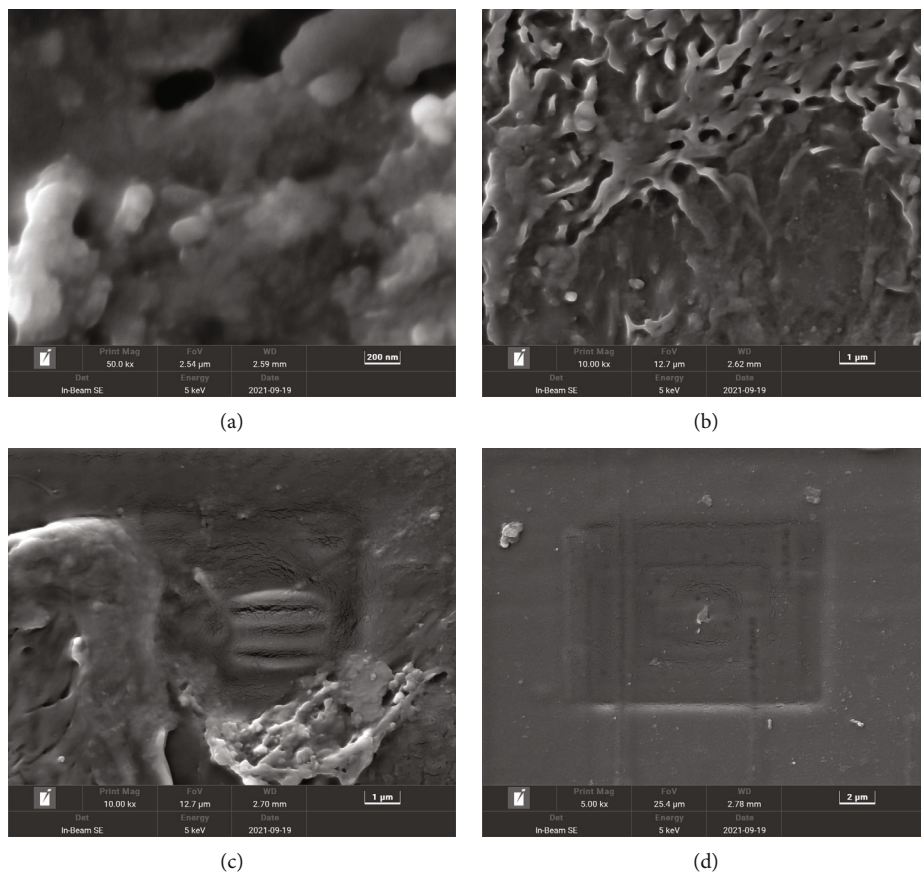


FIGURE 1: SEM images of PVA biocomposite films: (a) PVA film; (b) PVA/5%CNCs; (c) PVA/5%CNCs/8%TA; (d) PVA/5%CNCs/8%TA/10%CS.

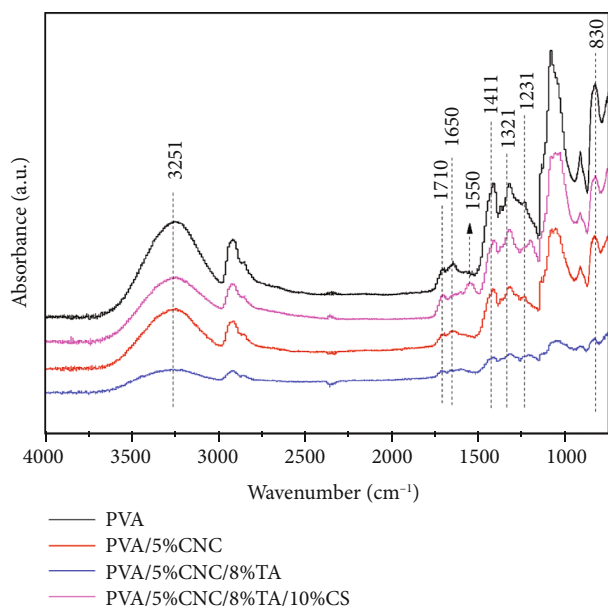


FIGURE 2: FTIR spectra of pure PVA and CNC-, TA-, and CS-modified biocomposite PVA films.

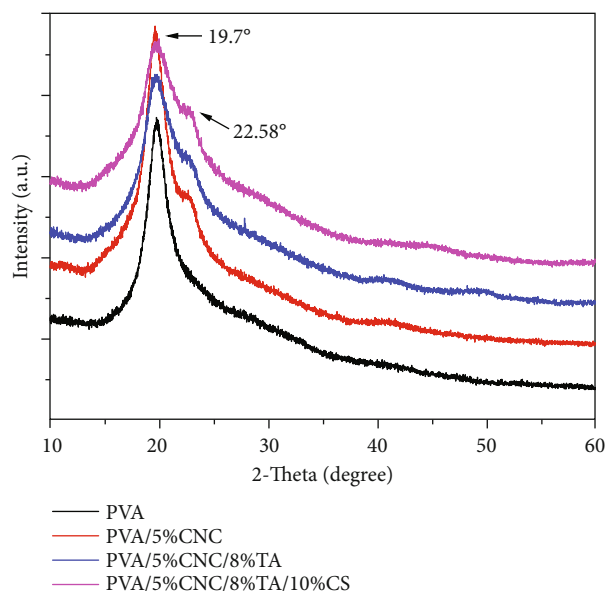


FIGURE 3: X-ray diffraction patterns of PVA films with or without CNCs, TA, and CS.

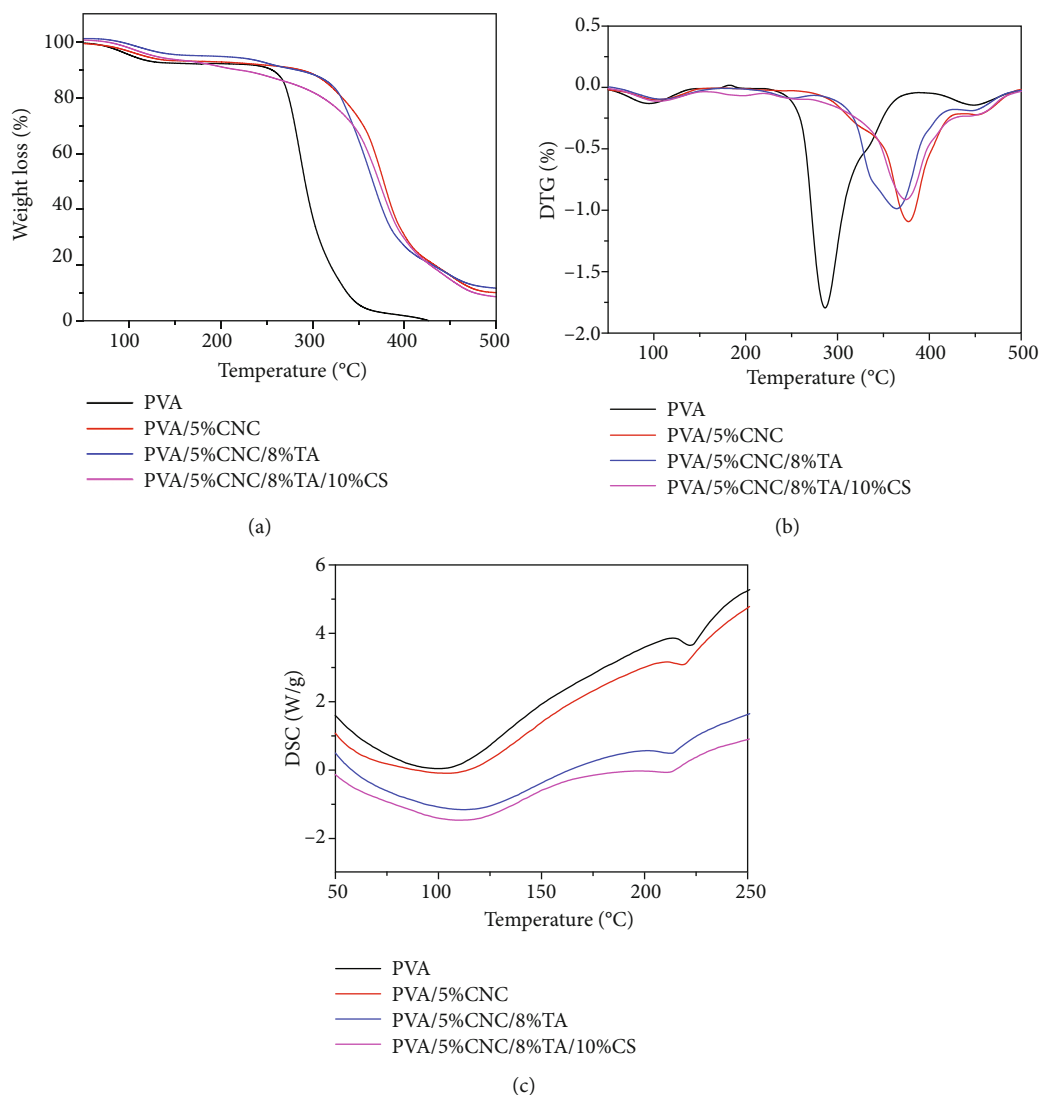


FIGURE 4: Thermal properties of PVA films with or without CNCs, TA, and CS: TG (a), DTG, (b) and DSC.

PVA films with 5% CNCs were further crosslinked by tannic acid. The tensile strength was improved remarkably from 66.1 MPa to 75.5 MPa with increasing tannic acid from 2% to 10%. The elongation at break was similarly increased first from 14.3% to 54.8% as tannic acid increased from 2% to 8%. It was abruptly reduced to 5.4% when the tannic acid content reached 10%. The tannic acid had a large amount of oxygen functional groups, which could develop a strong crosslink among PVA, CNCs, and tannic acid by forming hydrogen bonds [32]. However, the excessive tannic acid would undermine its distribution in the PVA matrix, resulting in the weakness of elongation at break [30]. Therefore, 8% of tannic acid was optimized as the crosslinker dosage in this work.

Chitosan was selected as an antibacterial agent to improve the antibacterial activity of the resulting PVA films. As shown in Table 1, the addition of chitosan reduced the tensile strength and elongation at break of PVA films as compared with other PVA films without chitosan. With increasing chitosan contents from 5% to 20%, the tensile

strength of biocomposite PVA films was improved from 55.9 MPa to 63.0 MPa, while the elongation at break was reduced significantly from 33.9% to 2.0%. The decreasing tensile strength was influenced by the high concentration of gallic acid [33]. Excessive chitosan had changed the inner film structure resulting in the cliff fall of elongation at break [28]. With comprehensive consideration, 10% of CS was optimized to obtain acceptable mechanical properties of resulting PVA films.

**3.2. SEM Images.** SEM images in Figure 1 demonstrated the morphology and cross section of the biocomposite PVA films. The pure PVA film exhibited many layered channels with a few pores and cracks, interrupting the inner structure of film (Figure 1(a)), therefore reducing the tensile strength and elongation at break [33]. CNCs brought a positive change to structure, resulting in a stronger interaction and adhesion between the polymer matrix and the surface of CNCs [34]. Adding tannic acid to this system also brought amelioration in the morphological surface. Figure 1(c) shows

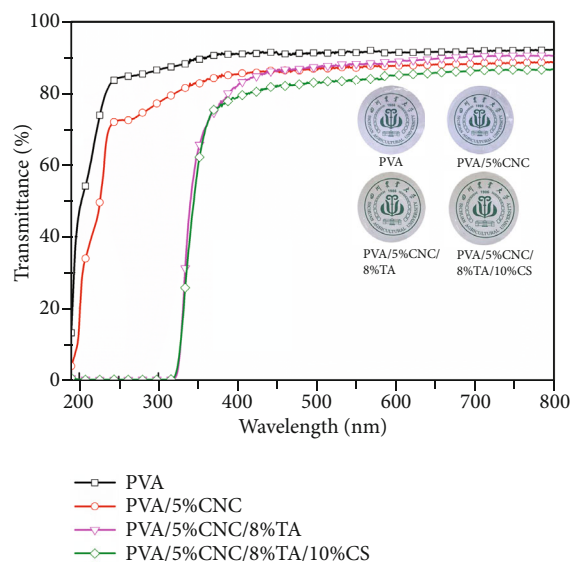


FIGURE 5: UV/vis spectroscopy analysis and light transmittance of biocomposite PVA with or without CNCs, TA, and CS.

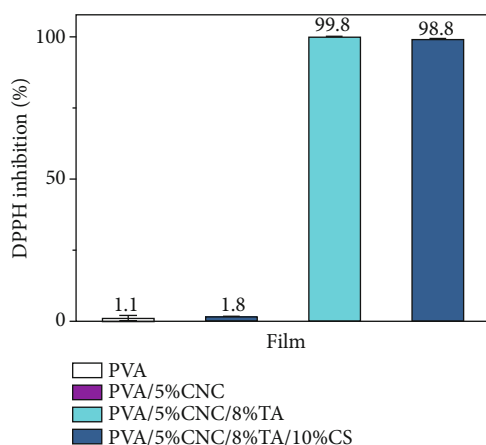


FIGURE 6: Inhibition activities of DPPH radical for biocomposite PVA films.

the biocomposite films containing tannic acid with a relatively homogeneous surface. It was worth noting the flat and smooth appearance of the PVA/CNC/TA/CS film in Figure 1(d), which was the mixture of these components. However, for those irregularity in films, we could expect them as indicators of the crosslinking points, and consequently better mechanical properties could be explained [20].

**3.3. FTIR Spectra.** The chemical structures of PVA films were examined through FTIR, as shown in Figure 2. The peak at  $3251\text{ cm}^{-1}$  was observed in all spectra, which was assigned to the free vibration of the hydroxyl groups, including intramolecular hydrogen bonds from PVA and intermolecular hydrogen bonding in hydroxyl groups of PVA [30]. The peaks at  $1321\text{ cm}^{-1}$  and  $1231\text{ cm}^{-1}$  were attributed to  $-\text{CO}$  groups in PVA [35]. The relative weaknesses in these peaks for films containing CNCs were ascribed to the strong hydrogen bond between PVA and CNCs [34]. Additionally,

the peak at  $830\text{ cm}^{-1}$  was assigned to the out-of-plane bending vibration of  $-\text{OH}$  groups in PVA, which decreased as nanocellulose, tannic acid, and chitosan gradually added. It evidenced the intermolecular interactions among CNCs, tannic acid, chitosan, and PVA [36]. The intensities of these peaks ( $3251\text{ cm}^{-1}$ ,  $1321\text{ cm}^{-1}$ ,  $1231\text{ cm}^{-1}$ , and  $830\text{ cm}^{-1}$ ) mentioned above weakened with the addition of CNCs, tannic acid, and chitosan, which elaborated the potential interaction among them [34, 37]. However, the spectrum of chitosan films exhibited a distinctive absorption peak at  $1550\text{ cm}^{-1}$  ( $-\text{NH}_2$  bending in primary amine), suggesting that the hydrogen bonding was formed between tannic acid and chitosan [38].

**3.4. X-Ray Diffraction.** As observed in Figure 3, all these films had a peak at around  $2\theta = 19.7^\circ$ , which was the characteristic peak of PVA [39]. It was known that the peak at  $19.7^\circ$  resulted from the strong intermolecular interaction in PVA chains through the intermolecular hydrogen bonding [40]. It was also observed that the addition of CNCs to PVA resulted in the highest peak at  $19.7^\circ$ , probably due to the interaction caused by strongly intermolecular hydrogen bonding between PVA and CNCs. The characteristic peaks of nanocellulose were predicted at  $2\theta = 12.58^\circ$  (for the 110 plane) and  $2\theta = 22.58^\circ$  (for the 200 plane) [30]. Tannic acid should display a broad peak at around  $2\theta = 25^\circ$  with some shoulders, and chitosan should have sharp peaks at  $2\theta = 11.4^\circ$  and  $22.6^\circ$  [41, 42]. However, all of them were absent in Figure 3 except for the peak at  $22.58^\circ$ , which belongs to CNCs. That was probably ascribed to the interaction among PVA, CNCs, tannic acid, and chitosan. Moreover, it also evidenced their even dispersions in the PVA matrix.

**3.5. Thermal Activities.** The TG, DTG, and DSC curves of PVA films are shown in Figure 4. The degradations of PVA films were divided into three main weight loss regions. The initial weight loss was 7% from  $63^\circ\text{C}$  to  $144^\circ\text{C}$ , which was ascribed to the loss of weak bound moisture and the absorbed water [30, 41, 43]. The main decomposition of all biocomposite PVA films occurred in the second region from  $235^\circ\text{C}$  to  $360^\circ\text{C}$ . This region involved the splitting of monomers and bond scission in the polymeric backbone [44]. According to Figure 4(b), the pure PVA film started to decompose earlier than other films, clearly proving that CNCs restricted the mobility of the polymer chain [45]. The biocomposite PVA films had lower weight loss rates than the pure PVA film (Figure 4(b)), which resulted from the enhancement of the crosslink between PVA and CNCs that influenced the mobility of polymer chains. As a result, the biocomposite PVA films presented obviously better thermal stabilities than the pure PVA film. The third weight loss stage started at around  $390^\circ\text{C}$ , predominating for the small quantities of hydrocarbon, which were the cleavage and decomposition of carbonaceous materials [46]. The pure PVA film had less residues than other biocomposite PVA films due to its less carbonaceous materials.

The DSC thermograms are presented in Figure 4(c). The analysis was performed by a heating-cooling-heating cycle. The broad endothermic peaks at about  $50^\circ\text{C}$  to  $125^\circ\text{C}$  were

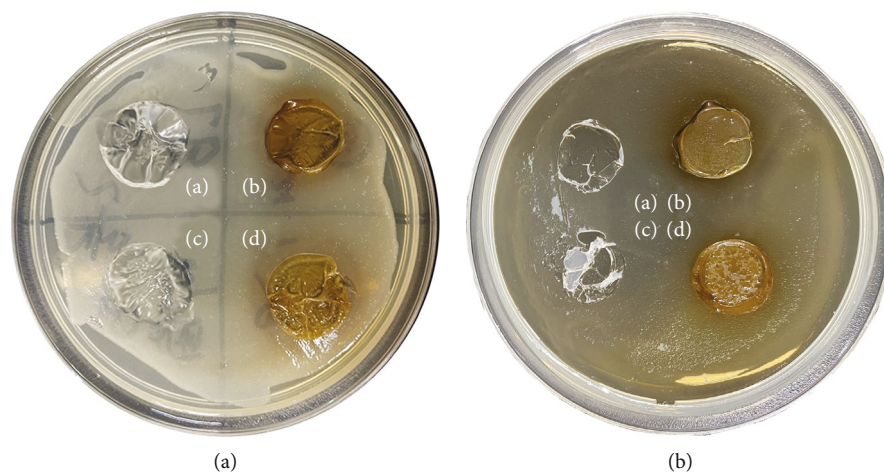


FIGURE 7: The antibacterial properties of biocomposite PVA films against (a) *Escherichia coli* and (b) *Staphylococcus aureus* (a: PVA; b: PVA/5%CNC/8%TA; c: PVA/5%CNC; and d: PVA/5%CNC/8%TA/10%CS).

ascribed to the water evaporation and residual acetic acid solvents used in the preparation of films [47]. The melting temperature of pure PVA (221°C) was higher than those of other three biocomposite PVA films at 218°C, 212°C, and 211°C, respectively. The results indicated that the addition of CNCs, tannic acid, and chitosan slightly lowered the melting temperature of the biocomposite PVA films.

**3.6. UV/Visible Spectra.** The results from UV-vis measurements of antiultraviolet properties and light transmittance are shown in Figure 5. The best transmittance was observed from the pure PVA film (93%). After introducing CNCs, tannic acid, and chitosan into the PVA matrix, lower transmittances were observed at 88%, 90%, and 86%, respectively. These decreases in transmittance indicated the uniform dispersion of additions in the PVA matrix [48].

The introduction of tannic acid led to powerfully antiultraviolet properties below 400 nm, especially in the short-wave ranging from 400 nm to 320 nm, while the pure PVA and PVA/CNCs films had poor abilities in ultraviolet absorbing. In a visible light wavelength region (>400 nm), all these films displayed a good light transmittance and there was no agglomeration revealed by the visual observation. The fantastic light transmittance was attributed to the highly uniformed CNC dispersion [49].

**3.7. Antioxidant Properties.** In Figure 6, the pure PVA film presented the DPPH inhibition of 1.1%, indicating that there was no antioxidant property in pure PVA. The PVA/5%CNC film also had similar result, with 1.8% in DPPH inhibition. As expected, biocomposite PVA films containing tannic acid dramatically increased DPPH inhibition, reaching at 99.8%. The absorbance decreased because DPPH was scavenged by tannic acid through donation of hydrogen from DPPH to form a stable one, also resulting in color changing from purple to yellow [50]. Similar result of the PVA/5%CNC/8%TA/10%CS film at 98.8% could be observed, which further evidenced the antioxidant properties of tannic acid for chitosan films [28]. As a result, the

releasing of antioxidant ability from biocomposite PVA films to wrapping food can be realized.

**3.8. Antibacterial Activities.** Figure 7 presents the antibacterial activities of PVA films against *Escherichia coli* and *Staphylococcus aureus*. PVA films with tannic acid (b) and chitosan (d) had prominent distinction in inhibition zones from others. The PVA film within chitosan had the best antibacterial properties, with the diameters of the inhibition zone about 24.4 mm and 22.1 mm, respectively. Similarly, the PVA film with 8% tannic acid also had good antibacterial activities with the diameter of the inhibition zone around 19.0 mm. Chitosan had antibacterial activity due to its cationic property [51]. The antimicrobial abilities of chitosan and tannic acid could be attributed to the interaction between molecules and cell membranes of bacteria, which resulted in the leakage of the inner organelles or the interruption of the metabolism of the bacteria [52]. The result also indicated that pure PVA (a) and PVA/5%CNC (c) films did not have antibacterial properties against *Escherichia coli* and *Staphylococcus aureus*.

## 4. Conclusion

The ecofriendly biocomposite PVA films reinforced by CNCs within an additional crosslinker (tannic acid) and antibacterial reagent (chitosan) were prepared, and their properties were evaluated and discussed in this work. Observation from the surface morphology of biocomposite PVA films showed that the PVA/CNC/TA/CS films were homogeneously dispersed structures. The results of FTIR and XRD evidenced the intense interactions and uniform dispersions of CNCs, tannic acid, and chitosan within the PVA matrix. The mechanical properties and thermal stabilities were remarkably improved after introducing CNCs and tannic acid into PVA. Besides, the biocomposite PVA films with tannic acid performed better antiultraviolet abilities than others, and all these biocomposite PVA films displayed a favorable light transmittance. Prominent antioxidant property of tannic acid made it possible for modified PVA films

to be used as active packaging materials. As an antibacterial agent, the addition of chitosan in PVA films presented the best antibacterial properties. Consequently, the enhanced physical and mechanical properties of biocomposite PVA films demonstrated their potential application in future food packaging markets.

### Data Availability

All data used to support the findings of this study are included within the article.

### Conflicts of Interest

The authors declare that they have no conflicts of interest.

### Authors' Contributions

Ruowen Tan and Feng Li are co-first authors.

### Acknowledgments

This work was supported by the Essential Scientific Research of Chinese National Non-profit Institute (CAFYBB2019ZB006, CAFYBB2018GB001), the Natural Science Foundation of China (No. 31770622), the Yunnan Applied Basic Research Projects (2019FA013), the Foundation of Key Laboratory of Pulp and Paper Science and Technology of Ministry of Education of China (KF201909), the Hainan Tropical Wildlife Park and Botanical Garden and the Project of Nanhai Series of Talent Cultivation Program, and the Research Start-up Fund on Talents Introduction in Sichuan Agricultural University.

### References

- [1] A. George, M. R. Sanjay, R. Srisuk, J. Parameswaranpillai, and S. Siengchin, "A comprehensive review on chemical properties and applications of biopolymers and their composites," *International Journal of Biological Macromolecules*, vol. 154, pp. 329–338, 2020.
- [2] R. J. Moon, A. Martini, J. Nairn, J. Simonsen, and J. Youngblood, "Cellulose nanomaterials review: structure, properties and nanocomposites," *Chemical Society Reviews*, vol. 40, no. 7, pp. 3941–3994, 2011.
- [3] D. S. Cha and M. S. Chinnan, "Biopolymer-based antimicrobial packaging: a review," *Critical Reviews in Food Science and Nutrition*, vol. 44, no. 4, pp. 223–237, 2004.
- [4] M. El Achaby, N. El Miri, A. Aboulkas et al., "Processing and properties of eco-friendly bio-nanocomposite films filled with cellulose nanocrystals from sugarcane bagasse," *International Journal of Biological Macromolecules*, vol. 96, pp. 340–352, 2017.
- [5] J. C. Grunlan, A. Grigorian, C. B. Hamilton, and A. R. Mehra, "Effect of clay concentration on the oxygen permeability and optical properties of a modified poly (vinyl alcohol)," *Journal of Applied Polymer Science*, vol. 93, no. 3, pp. 1102–1109, 2004.
- [6] C. C. DeMerlis and D. R. Schoneker, "Review of the oral toxicity of polyvinyl alcohol (PVA)," *Food and Chemical Toxicology*, vol. 41, no. 3, pp. 319–326, 2003.
- [7] H. Tian and H. Tagaya, "Dynamic mechanical property and photochemical stability of perlite/PVA and OMMT/PVA nanocomposites," *Journal of Materials Science*, vol. 43, no. 2, pp. 766–770, 2008.
- [8] V. Sedlářik, N. Saha, I. Kuřitka, and P. Saha, "Characterization of polymeric biocomposite based on poly (vinyl alcohol) and poly (vinyl pyrrolidone)," *Polymer Composites*, vol. 27, no. 2, pp. 147–152, 2006.
- [9] X. Tang and S. J. Alavi, "Recent advances in starch, polyvinyl alcohol based polymer blends, nanocomposites and their biodegradability," *Carbohydrate Polymers*, vol. 85, no. 1, pp. 7–16, 2011.
- [10] L. Marinescu, D. Ficai, O. Oprea et al., "Optimized synthesis approaches of metal nanoparticles with antimicrobial applications," *Journal of Nanomaterials*, vol. 2020, 14 pages, 2020.
- [11] Y. Habibi, L. A. Lucia, and O. J. Rojas, "Cellulose nanocrystals: chemistry, self-assembly, and applications," *Chemical Reviews*, vol. 110, no. 6, pp. 3479–3500, 2010.
- [12] I. Capron, O. J. Rojas, and R. Bordes, "Behavior of nanocelluloses at interfaces," *Current Opinion in Colloid & Interface Science*, vol. 29, pp. 83–95, 2017.
- [13] F. Ferreira, A. Dufresne, I. Pinheiro et al., "How do cellulose nanocrystals affect the overall properties of biodegradable polymer nanocomposites: a comprehensive review," *European Polymer Journal*, vol. 108, pp. 274–285, 2018.
- [14] X. Li, J. Li, J. Gong, Y. Kuang, L. Mo, and T. Song, "Cellulose nanocrystals (CNCs) with different crystalline allomorph for oil in water Pickering emulsions," *Carbohydrate Polymers*, vol. 183, pp. 303–310, 2018.
- [15] H. Lee, J. You, H. J. Jin, and H. W. Kwak, "Chemical and physical reinforcement behavior of dialdehyde nanocellulose in PVA composite film: a comparison of nanofiber and nanocrystal," *Carbohydrate Polymers*, vol. 232, p. 115771, 2020.
- [16] N. Noshirvani, W. Hong, B. Ghanbarzadeh, H. Fasihi, and R. Montazami, "Study of cellulose nanocrystal doped starch-polyvinyl alcohol bionanocomposite films," *International Journal of Biological Macromolecules*, vol. 107, no. Part B, pp. 2065–2074, 2018.
- [17] E. Sharmin, S. Ahmad, and F. J. Zafar, "Renewable resources in corrosion resistance," in *Corrosion Resistance*, IntechOpen, 2012.
- [18] N. Sahiner, S. Sagbas, M. Sahiner, C. Silan, N. Aktas, and M. Turk, "Biocompatible and biodegradable poly(tannic acid) hydrogel with antimicrobial and antioxidant properties," *International Journal of Biological Macromolecules*, vol. 82, pp. 150–159, 2016.
- [19] T. S. Sileika, D. G. Barrett, R. Zhang, K. H. A. Lau, and P. B. J. Messersmith, "Colorless multifunctional coatings inspired by polyphenols found in tea, chocolate, and wine," *Angewandte Chemie International Edition*, vol. 52, no. 41, pp. 10766–10770, 2013.
- [20] S. Rivero, M. A. García, and A. Pinotti, "Crosslinking capacity of tannic acid in plasticized chitosan films," *Carbohydrate Polymers*, vol. 82, no. 2, pp. 270–276, 2010.
- [21] X. Zhang, M. D. Do, P. Casey et al., "Chemical modification of gelatin by a natural phenolic cross-linker, tannic acid," *Journal of Agricultural and Food Chemistry*, vol. 58, no. 11, pp. 6809–6815, 2010.
- [22] K. H. Hong, "Polyvinyl alcohol/tannic acid hydrogel prepared by a freeze-thawing process for wound dressing applications," *Polymer Bulletin*, vol. 74, no. 7, pp. 2861–2872, 2017.

- [23] I. Arvanitoyannis, I. Kolokuris, A. Nakayama, N. Yamamoto, and S.-i. Aiba, "Physico-chemical studies of chitosan-poly(vinyl alcohol) blends plasticized with sorbitol and sucrose," *Carbohydrate Polymers*, vol. 34, no. 1-2, pp. 9-19, 1997.
- [24] M. E. I. Badawy and E. I. Rabea, "Synthesis and antifungal property of N-(aryl) and quaternary N-(aryl) chitosan derivatives against *Botrytis cinerea*," *Cellulose*, vol. 21, no. 4, pp. 3121-3137, 2014.
- [25] X. Fei Liu, Y. Lin Guan, D. Zhi Yang, Z. Li, and K. De Yao, "Antibacterial action of chitosan and carboxymethylated chitosan," *Journal of Applied Polymer Science*, vol. 79, no. 7, pp. 1324-1335, 2001.
- [26] P. Sahariah and M. J. Masson, "Antimicrobial chitosan and chitosan derivatives: a review of the structure-activity relationship," *Biomacromolecules*, vol. 18, no. 11, pp. 3846-3868, 2017.
- [27] A. K. Patel, R. Bajpai, and J. M. Keller, "On the crystallinity of PVA/palm leaf biocomposite using DSC and XRD techniques," *Microsystem Technologies*, vol. 20, no. 1, pp. 41-49, 2014.
- [28] J. Liu, S. Liu, Q. Wu, Y. Gu, J. Kan, and C. J. Jin, "Effect of protocatechuic acid incorporation on the physical, mechanical, structural and antioxidant properties of chitosan film," *Food Hydrocolloids*, vol. 73, pp. 90-100, 2017.
- [29] M. R. Kamal and V. Khoshkava, "Effect of cellulose nanocrystals (CNC) on rheological and mechanical properties and crystallization behavior of PLA/CNC nanocomposites," *Carbohydrate Polymers*, vol. 123, pp. 105-114, 2015.
- [30] A. Mandal and D. J. Chakrabarty, "Studies on the mechanical, thermal, morphological and barrier properties of nanocomposites based on poly(vinyl alcohol) and nanocellulose from sugarcane bagasse," *Journal of Industrial Engineering Chemistry*, vol. 20, no. 2, pp. 462-473, 2014.
- [31] V. Khoshkava and M. J. Kamal, "Effect of drying conditions on cellulose nanocrystal (CNC) agglomerate porosity and dispersibility in polymer nanocomposites," *Powder Technology*, vol. 261, pp. 288-298, 2014.
- [32] M.-Y. Lim, H. Shin, D. M. Shin, S.-S. Lee, and J.-C. J. Lee, "Poly(vinyl alcohol) nanocomposites containing reduced graphene oxide coated with tannic acid for humidity sensor," *Polymer Bulletin*, vol. 84, pp. 89-98, 2016.
- [33] X. Sun, Z. Wang, H. Kadouh, and K. J. Zhou, "The antimicrobial, mechanical, physical and structural properties of chitosan-gallic acid films," *LWT-Food Science and Technology*, vol. 57, no. 1, pp. 83-89, 2014.
- [34] K. Choo, Y. C. Ching, C. H. Chuah, S. Julai, and N. S. Liou, "Preparation and characterization of polyvinyl alcohol-chitosan composite films reinforced with cellulose nanofiber," *Materials (Basel)*, vol. 9, no. 8, p. 644, 2016.
- [35] H. S. Mansur, C. M. Sadahira, A. N. Souza, and A. A. J. Mansur, "FTIR spectroscopy characterization of poly(vinyl alcohol) hydrogel with different hydrolysis degree and chemically crosslinked with glutaraldehyde," *Materials Science Engineering: C*, vol. 28, no. 4, pp. 539-548, 2008.
- [36] M. S. Peresin, Y. Habibi, J. O. Zoppe, J. J. Pawlak, and O. J. Rojas, "Nanofiber composites of polyvinyl alcohol and cellulose nanocrystals: manufacture and characterization," *Biomacromolecules*, vol. 11, no. 3, pp. 674-681, 2010.
- [37] H. M. P. Naveen Kumar, M. N. Prabhakar, C. Venkata Prasad et al., "Compatibility studies of chitosan/PVA blend in 2% aqueous acetic acid solution at 30 °C," *Carbohydrate Polymers*, vol. 82, no. 2, pp. 251-255, 2010.
- [38] A. Sionkowska, B. Kaczmarek, and K. J. Lewandowska, "Modification of collagen and chitosan mixtures by the addition of tannic acid," *Journal of Molecular Liquids*, vol. 199, pp. 318-323, 2014.
- [39] M. S. Islam, M. S. Rahaman, and J. H. Yeum, "Electrospun novel super-absorbent based on polysaccharide-polyvinyl alcohol-montmorillonite clay nanocomposites," *Carbohydrate Polymers*, vol. 115, pp. 69-77, 2015.
- [40] X.-f. Qian, J. Yin, S. Feng, S.-h. Liu, and Z.-k. Zhu, "Preparation and characterization of polyvinylpyrrolidone films containing silver sulfide nanoparticles," *Journal of Materials Chemistry*, vol. 11, no. 10, pp. 2504-2506, 2001.
- [41] A. Mandal and D. J. Chakrabarty, "Isolation of nanocellulose from waste sugarcane bagasse (SCB) and its characterization," *Carbohydrate Polymers*, vol. 86, no. 3, pp. 1291-1299, 2011.
- [42] H. Dai, Y. Huang, and H. Huang, "Enhanced performances of polyvinyl alcohol films by introducing tannic acid and pineapple peel-derived cellulose nanocrystals," *Cellulose*, vol. 25, no. 8, pp. 4623-4637, 2018.
- [43] M.-J. Cho and B.-D. Park, "Tensile and thermal properties of nanocellulose-reinforced poly(vinyl alcohol) nanocomposites," *Journal of Industrial and Engineering Chemistry*, vol. 17, no. 1, pp. 36-40, 2011.
- [44] G. Attia and M. F. H. Abd El-kader, "Structural, optical and thermal characterization of PVA/2HEC polyblend films," *International Journal of Electrochemical Science*, vol. 8, no. 4, pp. 5672-5687, 2013.
- [45] M. Abdelaziz, "Cerium (III) doping effects on optical and thermal properties of PVA films," *Physica B: Condensed Matter*, vol. 406, no. 6-7, pp. 1300-1307, 2011.
- [46] L. T. Sin, W. Rahman, A. Rahmat, and M. J. Mokhtar, "Determination of thermal stability and activation energy of polyvinyl alcohol-cassava starch blends," *Carbohydrate Polymers*, vol. 83, no. 1, pp. 303-305, 2011.
- [47] V. A. Pereira Jr., I. N. Q. de Arruda, and R. J. Stefani, "Active chitosan/PVA films with anthocyanins from *Brassica oleracea* (red cabbage) as time-temperature indicators for application in intelligent food packaging," *Food Hydrocolloids*, vol. 43, pp. 180-188, 2015.
- [48] M. Yadav and F. C. Chiu, "Cellulose nanocrystals reinforced  $\kappa$ -carrageenan based UV resistant transparent bionanocomposite films for sustainable packaging applications," *Carbohydrate Polymers*, vol. 211, pp. 181-194, 2019.
- [49] E. Fortunati, D. Puglia, F. Luzi, C. Santulli, J. M. Kenny, and L. Torre, "Binary PVA bio-nanocomposites containing cellulose nanocrystals extracted from different natural sources: part I," *Carbohydrate Polymers*, vol. 97, no. 2, pp. 825-836, 2013.
- [50] İ. Gülçin, Z. Huyut, M. Elmastaş, and H. Y. Aboul-Enein, "Radical scavenging and antioxidant activity of tannic acid," *Arabian Journal of Chemistry*, vol. 3, no. 1, pp. 43-53, 2010.
- [51] A. B. Perumal, P. S. Sellamuthu, R. B. Nambiar, and E. R. J. Sadiku, "Development of polyvinyl alcohol/chitosan bionanocomposite films reinforced with cellulose nanocrystals isolated from rice straw," *Applied Surface Science*, vol. 449, pp. 591-602, 2018.
- [52] F. Devlieghere, A. Vermeulen, and J. Debever, "Chitosan: antimicrobial activity, interactions with food components and applicability as a coating on fruit and vegetables," *Food Microbiology*, vol. 21, no. 6, pp. 703-714, 2004.